The influence of axial compressive stresses on the formability and scattering of process parameters in micro-hydroforming processes of tubes

Christoph Hartl[a], Andreas Chlynin, and Max Radetzky

Cologne University of Applied Sciences Cologne, Betzdorfer Strasse 2, 50679 Cologne, Germany

Abstract. Feasible product geometries manufactured with micro-hydroforming, as well as process stability are crucially influenced by the microstructure of the used tube material. The higher ratio of grain size to tube wall thickness d_k/t_0 in micro-hydroforming, compared to conventional tube hydroforming, leads to an increase of scattering of process parameters and instabilities. This paper presents experimental and theoretical results for the micro-hydroforming of tubes made from stainless steel and from platinum with a focus on the correlations between the microstructure of the workpiece material, the stress state during forming and the resulting stability of the forming process. Investigated tube dimensions were 800 μm outer diameter and 40 μm wall thickness of the steel tubes, respectively 1650 μm and 76 μm of the platinum tubes. The average ratio d_k/t_0 was about 0.3 for the steel material and about 0.9 for the platinum alloy. It has been shown that superimposed axial stresses are suitable to reduce the restricting influence of an increased ratio d_k/t_0 and to improve the forming result as well as the process stability.

1. Introduction

Micro-Hydroforming is a down-scaled forming process, based on the expansion of metal tubes with outer diameters below about 1000 μm by internal pressurization within a die cavity which corresponds to the final workpiece shape. It was developed to provide an economic technology for the mass production of complex hollow shaped components at micro-scale for the strong demand from numerous industrial sectors on the field of micro-technology. [1, 2]. In particular the medical market is characterized by a use of tubular micro-products which show a great potential to be manufactured by micro-hydroforming.

Similar to other micro-forming processes, so-called size-effects [3] influence the feasible product geometry with micro-hydroforming as well as the process stability. An important cause of size-effects is resulting from the increasing ratio of grain size to tube wall thickness d_k/t_0 in micro-hydroforming when reducing the scale compared to conventional tube hydroforming process size. Experimental bursting tests of micro-tubes and the comparison of the results with tests of macro-tubes in [4] have shown that such influences have to be considered in micro-hydroforming.

The reason for this was provided with the work of [5], where it was shown theoretically by the use of a plain strain crystal plasticity finite element based modelling technique that localized necking of a

---

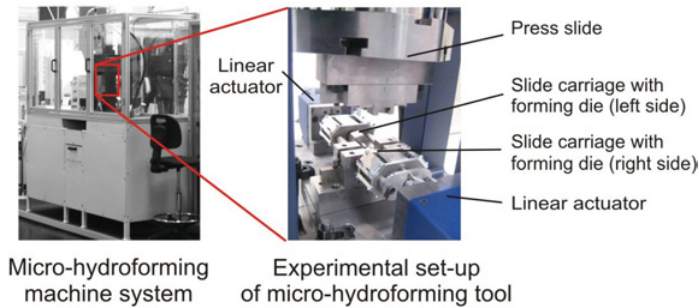[a] Corresponding author: `christoph.hartl@fh-koeln.de`

Figure 1. Micro-Hydroforming machine system [1, 8].

micro-tube wall is related to the angle between the crystal slip systems and the hoop stress direction. Consequently, as a result of the small number of grains in tube wall direction, necking and following bursting progresses faster in the expansion of micro-tubes than in macro-tubes which can be regarded as a homogeneous continuum due to their larger number of grains.

For conventional hydroforming it has already been identified that a superimposed axial compressive force improves the formability of the tube metal [6]. This measure reduces the occurrence of instabilities due to necking at an early stage of the process in so far as no other instabilities ensues, caused by an excessive axial force such as wrinkling or buckling of the tube [6]. A first experimental application of axial forces in micro-hydroforming have been already presented by [7] with the objective to investigate suitable sealing systems for the forming of tubes with an outer diameter of 1000 μm. However, until now no systematic research has been published concerning the influences of superimposed axial forces on the formability for micro-hydroforming processes.

The present paper summarizes experimental results for the micro-hydroforming of tubes made from stainless steel AISI 304 [4] and from the platinum alloy PtIr10 [8], in conjunction with their analysis with the aid of finite element simulations (FEA). Special focus is on the correlations between the microstructure of the workpiece material, the stress state during forming with and without the application of superimposed axial forces and the resulting stability of the forming process.

2. Experimental set-up

The micro-hydroforming machine system shown in Fig. 1 was used to conduct the experimental work [1]. It is applicable for the micro-hydroforming of components with cross section dimensions between about 200 μm and 2000 μm and is equipped with a spindle driven pressure intensifier which enables to apply an internal pressure p_i of up to 400 MPa. The machine system is provided with three axes for a translatory movement of tool elements: Two linear actuators with spindle gears with a maximum force F_a of 800 N, and one hydraulic driven actuator with a maximum force F_c of 20 kN. The machine is equipped with a flexible control system based on a conventional programmable logic controller system.

The starting tubes used for the experiments were provided in annealed condition with the measured dimensions and mechanical specifications determined by tensile tests of the tubular material as listed in Table 1. To expand the micro-tubes made from AISI 304, the tube ends were clamped without a possible axial movement and pressurized with increasing p_i, until instability due to necking and subsequent bursting occurred, as described in [4].

The experimental results for the tubes made from PtIr10 are an outcome of a feasibility study, documented in [8], where from a total number of approximately 300 experimental trials those tests were analysed which showed failures due to necking and bursting of the tube wall. Two types of load

Table 1. Material properties and dimensions of the hydroformed micro-tubes.

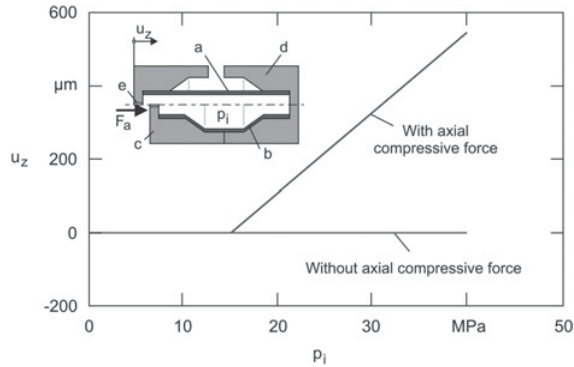|	Stainless steel tubes	Platinium tubes
Material	AISI 304	PtIr10
Initial yield stress σ_{Y0} (MPa)	329	250
Tensile strength σ_{UTS} (MPa)	699	346
Tube outer diameter d_0 (µm)	799	1651
Tube wall thickness t_0 (µm)	39	76
Tube length l_0 (mm)	10	8

Figure 2. Load paths for platinum tube expansion (a) starting tube, b) hydroformed component, c) left tool half, d) right tool half, e) inlet for pressurizing medium).

paths were applied to these tubes: the first type with only the internal pressure p_i as a forming load for the expansion, with the tube ends clamped by the sealing system, and a second with expansion by p_i and a superimposed axial compressive force F_a, caused by an axial stroke u_z of the left half of the tools. Figure 2 shows the schematic tool set-up and applied load paths.

3. Modelling of finite element simulations

To support the analysis of the experimental results, FE-models of the hydroforming tests were developed, based on a two dimensional, axisymmetric approach. The software ABAQUS with an explicit algorithm was applied to compute the finite element based simulation model which consisted of about 400 elements. 4-node, linear, axisymmetric elements of the type CAX4R were used. The symmetry of the forming process enabled to simplify the model and to calculate merely one halve of the formed component. Furthermore, the part of the tube end located in the tool area where the die cavity dimension corresponds to the outer tube diameter was not included in the model. In this area no notable change in the wall thickness was measured at the experimentally formed components. Hence, material movement and relative movement between the outer surface of the tube end and the tool surface in this area were negligible in the present case. The internal pressure p_i was applied as a normal stress to the inner surface of the tube model and the axial stroke u_z was implemented by an according displacement of the outer element nodes in the sectional plane of the model as depicted in Fig. 3a. For the simulations without axial compression force, an axial stroke of $u_z = 0$ was applied.

Homogenous and isotropic elastic-plastic material behaviour with strain hardening was applied in order to establish the ideal forming process without size-effects, according to the material properties
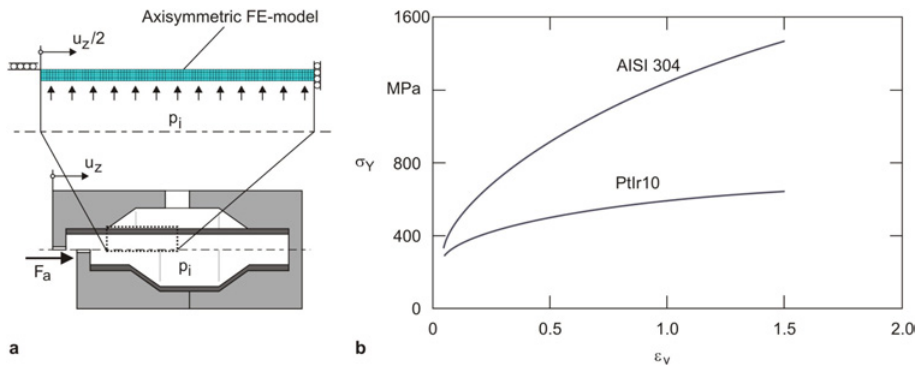
Figure 3. FE-modelling, a) diagram of the model for FE-simulations, b) approximated yield curves of the investigated materials with yield stress σ_Y versus plastic equivalent strain ε_v.
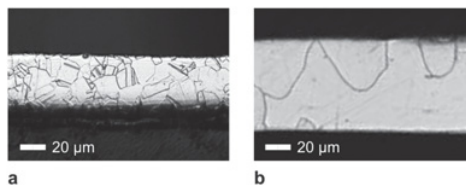

Figure 4. Microstructure of the workpiece materials, a) stainless steel tube (AISI 304), b) platinum tube (PtIr10).

presented in Table 1 and with the yield curves as provided by [9] (Fig. 3b). Upsetting tests of cylindrical specimens were conducted to determine the yield curves.

4. Results

The microstructure of the starting tubes was analysed (Fig. 4) and an average grain size d_k of 12 μm for the stainless steel tube material and 68 μm for the platinum tube material was determined. This results in grain size to wall thickness ratios d_k/t_0 of 0.3 and 0.9 respectively. In both cases the grains were equally shaped and randomly orientated without a visible texture. The number of single grains with $d_k/t_0 \approx 1$ was considerably higher for the platinum tubes compared to the workpieces made from stainless steel.

For both types of tubes, the expansion under the applied loads was calculated with the simulation model described before. Figure 5 shows the acting internal pressure p_i versus the radial expansion r_x of the tube wall at the maximum point of expansion. Furthermore, the experimentally measured internal pressures for the occurrence of a failure were collected and marked in these diagrams. For the experiments with the stainless steel micro-tubes, measurement data for r_x were derived from the analysed average expansion diameter at bursting [4] and considered in Fig. 5a. The positions of the failure cases along the simulated p_i-r_x-curve for the platinum tubes (Fig. 5b) were obtained by projecting the experimentally measured internal pressures at bursting to this curve.

The expansion tests of the stainless steel tubes delivered a scattering of the internal pressure for the occurrence of bursting between 55.7 and 57.4 MPa which corresponds to a standard deviation of 0.55 MPa. A considerably higher scattering was determined for the experiments with the platinum tubes. In particular for those, which were formed without superimposed axial force. For these tests, the lowest value of bursting pressure was determined with 11 MPa, and the highest with 39 MPa. The bursting pressures for the trials with axial compressive force were between 32 and 38.9 MPa. The resulting standard deviations are 9.4 MPa and 2.2 MPa respectively. It is evident in Fig. 5b that for the forming of
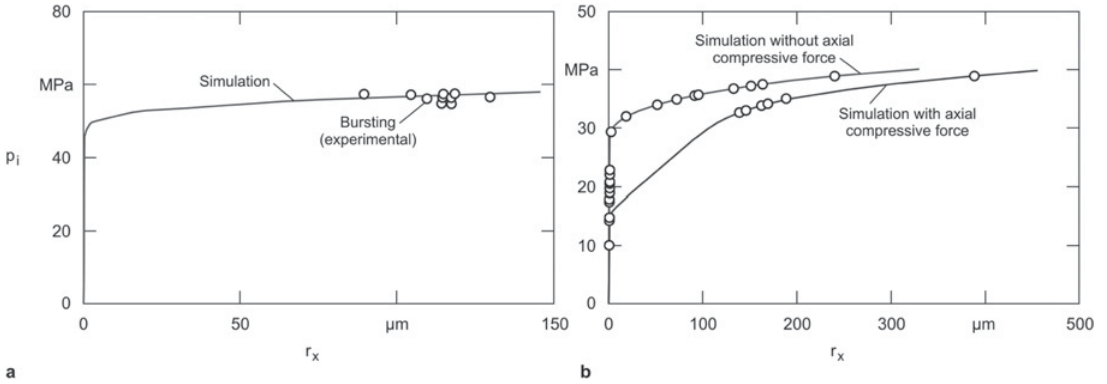
Figure 5. Pressure-expansion curves derived from simulations and experimentally determined bursting pressures, a) stainless steel tube (AISI 304), b) platinum tube (PtIr10).
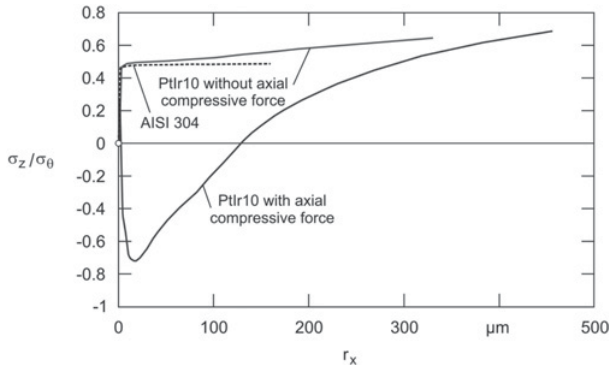

Figure 6. Simulation results of stress-ratio σ_z/σ_θ versus radial expansion r_x.

the platinum tubes without axial compressive force a considerable number of failures took place before the tubes started to expand. In the cases of the forming of stainless tubes with smaller ratio of grain size to wall thickness and the forming of the platinum tubes with superimposed axial compressive force, failures appeared only at higher internal pressures, when a noticeable expansion took place. The average maximum expansion diameter of the platinum tubes could be increased from about 1800 μm without superimposed axial force to about 1970 μm with applying an axial force.

It can be assumed that the premature bursting before the theoretical yield start of the expanded tubes made from PtIr10 was caused by the effect described in [5] which results from a comparatively large ratio of material grain size to wall thickness d_k/t_0. In cases where single huge grains are oriented with their crystal slip systems to the hoop stress direction in such a way that the resulting shear stress to move the lattice planes against each other is smaller than the respective shear stress of adjacent grains, local necking and subsequent bursting occur earlier in comparison with homogenous macro-tubes with a larger number of grains. Figure 6 presents the development of the ratio of axial stresses σ_z to hoop stresses σ_θ in the tube wall at the point of maximum expansion during the forming. It can be seen from this figure that the load paths applied to the tubes made from stainless steel and platinum, which do not provide a superimposed axial force, result in a stress ratio $\sigma_z/\sigma_\theta > 0$ along the overall forming process. In contrast to this, a superimposed axial compressive force is resulting in a stress ratio $\sigma_z/\sigma_\theta < 0$ at the
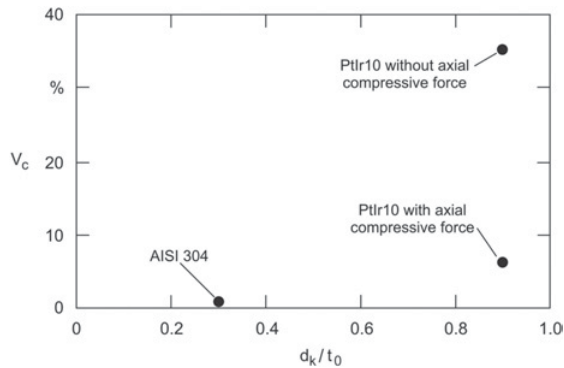
Figure 7. Coefficient of variation V_c versus grain size to wall thickness ratio d_k/t_0 for the investigated failure cases in micro-tube hydroforming expansions.

first stage of the process, which change at a radial expansion r_x of about 130 µm to $\sigma_z/\sigma_\theta > 0$ at the last stage (Fig. 6). This is resulting from the fact that at this point the amount of axial tensile stress, caused by the internal pressurization, is exceeding the amount of axial compressive stress, initiated by the superimposed axial compressive force.

The comparison of the development of the simulated stress states in Fig. 6 with the experimental occurrence of failures in Fig. 5 shows that in the case of a superimposed axial compressive force, failures appeared only after the point where the resulting stress ratio σ_z/σ_θ within the tube wall changed from negative to positive values. The fact that size-effects due to the large ratio of grain size to tube wall thickness increase the danger of premature necking and bursting, and that none of these failures was determined for the investigated samples within the area of $\sigma_z/\sigma_\theta < 0$, leads to the recommendation that a superimposed axial compressive force should be applied in micro-hydroforming of a maximum feasible amount within the limits of wrinkling and buckling of the tube wall. Figure 7 summarizes the results by comparing the coefficient of variation resulting from the standard deviation and average value of the determined internal pressures at occurrence of failures. It is obvious from this figure that small ratios of grain size to tube wall thickness and the application of superimposed axial forces contribute to a higher process stability and reduced scattering.

5. Conclusions

In this work, investigations about the the occurrence of failures caused by localised necking and following bursting in micro-hydroforming of tubes made from stainless steel and platinum is presented. Load paths for the hydroforming of the specimens were applied taking into account both forming with and without a superimposed axial compression force. In both cases, the measured values of the internal pressures in the event of instabilities showed a distinct scattering, with however a reduced deviation between the individual test results for the hydroforming with a superimposed axial force. Furthermore, the application of an axial compression force avoided the premature bursting of the formed tubes below the theoretical yield limit, which was detected for a considerable number of the expansion tests without axial force. Additionally, the feasible expansion diameter was increased. With the aid of finite element simulations it was found that, within the frame of the investigated process parameters and number of specimens, no failures occurred as long as axial compressive stresses were acting within the formed tube wall. An analysis of the microstructure of the tube material used showed an increasing scattering with increasing ratio of grain size to tube wall thickness. It was concluded that the scattering of the measured

internal pressure at the occurrence of failures can be attributed to the size-effects resulting from the amount of this ratio.

References

[1] C. Hartl, G. Anyasodor, Steel Research Int. **81**, 9 (2010)

[2] Y. Qin, A. Brockett, Y. Ma, J. Zhao, C. Harrison, W. Pan, X. Dai, D. Loziak, Int. J. Adv. Manuf. Technol. **47** (2010)

[3] F. Vollertsen, D. Biermann, H.H. Hansen, I.S. Jawahir, K. Kuzman, CIRP Annals **58**, 2 (2009)

[4] C. Hartl, G. Anyasodor, J. Lungershausen, in Proc. of Int. ESAFORM Conf. Metal Forming 2011, Belfast (2011)

[5] W. Zhuang, S. Wang, J. Lin, D. Balint, C. Hartl, Europ. J. Mechanics A/Solids **31** (2011)

[6] F. Dohmann, in Umformtechnik, edited by K. Lange, vol. 4 (Springer, Berlin, 1993)

[7] G. Ngaile, J. Lowrie, J. Micro Nano-Manuf. **2**, 4 (2014)

[8] C. Hartl, H. Schiefer, A. Chlynin, Manufacturing Rev. **1**, 17 (2014)

[9] N.N., VDI-Standard 3200, Issue 3 (The Association of German Engineers, Beuth, Berlin, 1982)